PAPER

Promoting effects of H_2 on photooxidation of volatile organic pollutants over Pt/TiO_2

Yilin Chen, Danzhen Li, Xinchen Wang, Ling Wu, Xuxu Wang and Xianzhi Fu*

Research Institute of Photocatalysis, Chemistry & Chemical Engineering College, Fuzhou University, Fuzhou 350002, P. R. China. E-mail: xzfu@fzu.edu.cn; Fax: +86-591-83738608; Tel: +86-591-83738608

Received (in Durham, UK) 1st August 2005, Accepted 21st September 2005
First published as an Advance Article on the web 10th October 2005

Superior photocatalytic activity and durability of Pt/TiO_2 for decomposing volatile organic pollutants (typically aromatic compounds) have been obtained by adding trace H_2 into an O_2-rich photooxidation system. The order of photodegradation efficiencies for volatile organic compounds is cyclohexane < acetone < benzene < toluene < ethylbenzene. Exceptional stability of Pt/TiO_2 for benzene photodegradation is still maintained after 22 h of testing, by the repeated use of the catalyst four times. The promoting effects of H_2 in the photocatalysis were studied by infrared spectroscopy (IR), spin-trapping electron paramagnetic resonance (EPR) and surface photovoltage spectroscopy (SPS). Results demonstrated that the introduced H_2 has several beneficial effects on heterogeneous photocatalysis, namely, a comparatively clean surface of Pt/TiO_2 with no persistent aromatic intermediates, an increased number of surface hydroxyl radicals in the photocatalytic process, and an enhanced separation efficiency of photogenerated electron–hole pairs. A mechanism is proposed to elucidate the promoting effect of H_2 on the photooxidation of volatile organic pollutants over Pt/TiO_2.

1. Introduction

Volatile organic compounds (VOCs), especially aromatic hydrocarbons, are widespread environmental pollutants emitted from numerous urban and industrial sources. Many of the VOCs are toxic, environmentally persistent, and some are considered to be carcinogenic, mutagenic, or teratogenic.[1] So far, a variety of advanced technologies has been developed for the efficient treatment of VOCs. Among these, TiO_2-based photocatalytic oxidation (PCO) is established to be one of the most promising technologies because it allows the complete decomposition of VOCs to the final products of CO_2 and H_2O at ambient conditions. Moreover, the oxidant used in PCO is environmentally-friendly: oxygen molecules.

However, one severe obstacle in the environmental application of photocatalysis is that the TiO_2 catalyst generally suffers from the limitation of relatively low quantum efficiency during the photocatalytic oxidation of VOCs.[2–6] In order to solve this problem, deposition of noble metals (*e.g.* Pt, Au, or Rh) on TiO_2 particles has been employed to improve the photocatalytic efficiency of TiO_2.[7–13] The improvement has been explained by a photoelectrochemical mechanism in which the noble metals act as a sink for photoinduced electrons, promoting the interfacial charge-transfer processes in the composite systems. Despite the beneficial effect of noble metal deposition, the photocatalyst still suffers from the limitation of poor durability during the treatment of stable aromatic compounds such as benzene at high concentrations.[14–16] The deactivation of the photocatalyst has been ascribed to the accumulation of stable intermediates on TiO_2 surfaces.[17] These intermediates block the surface active sites and subsequently deactivate the photocatalyst.

Recently, we have found that both photocatalytic activity and the stability of Pt/TiO_2 can be increased dramatically by adding a trace amount of hydrogen gas into the C_6H_6–O_2–Pt/TiO_2 photocatalytic system. The introduced H_2 increases the activity of Pt/TiO_2 for benzene photocatalytic oxidation by two orders of magnitude, as compared with that in the absence of H_2. In addition, no deactivation is observed during prolonged operation.[18] This surprising finding thus prompted us to study the role of H_2 during the photocatalytic processes on Pt/TiO_2 catalyst, and to explore the universality of this finding by extending the organic reactant from benzene to other VOCs.

Herein, the promoting effects of H_2 on the suppression of persistent reaction intermediates, the generation of active oxygen species, and the separation efficiency of photoinduced charge over a Pt/TiO_2 photocatalyst have been investigated by infrared spectra (IR), electron paramagnetic resonance (EPR), and surface photovoltage spectra (SPS). The physicochemical properties of the photocatalyst are also described. Benzene, toluene, ethylbenzene, cyclohexane, and acetone were chosen as probes for their high toxicity and structural stability. This also helped us to examine the applicability of the H_2–O_2–Pt/TiO_2 photocatalytic system for the decomposition of various VOCs.

2. Experimental section

2.1. Materials

Benzene (Acros, spectrophotometric grade) was purchased from the J&K Chemical Co. Hexachloroplatinic acid (Alfa, 99.95%) and silica (Alfa, specific surface = 144 $m^2\ g^{-1}$) were obtained from the Phentex Chemical Co. Titanium tetraisopropoxide and 5,5-dimethyl-1-pyrroline-*N*-oxide (DMPO) were purchased from the Sigma Chemical Co., provided in analytical grade and used without further treatment.

2.2. Catalyst preparation and characterization

A pure TiO_2 sample with particle sizes between 0.21 and 0.25 mm was prepared by calcining the sol-gel-derived TiO_2 xerogel at 623 K for 6 h.[19] No detectable IR absorption bands related

DOI: 10.1039/b510953a

to organic compounds were observed for the TiO_2 sample. A Pt/TiO_2 sample was prepared by impregnating the calcined TiO_2 with an aqueous solution of H_2PtCl_6. The initial ratio of Pt to TiO_2 was fixed at 1 wt%. The impregnated sample was dried at 383 K, and then calcined at 623 K for 3 h. The thus obtained solid was subsequently reduced with a $NaBH_4$ solution (0.1 M) to produce Pt/TiO_2.[14] XPS analysis of the final sample indicated that the Pt concentration on the TiO_2 surface was *ca.* 0.9 wt% and the valence state of most Pt was zero. A Pt/SiO_2 catalyst was prepared and used for comparison. The synthesis process of Pt/SiO_2 was similar to that of Pt/TiO_2.

X-Ray diffraction (XRD) analysis was performed using a Bruker D8 Advance diffractometer with Cu$K\alpha$ radiation. The crystallite size of anatase was calculated from the peak half-width by using the Scherrer equation with corrections for instrumental line broadening. Specific surface areas of the catalysts were determined by applying the BET method to the sorption of nitrogen at 77 K. UV-Vis diffuse reflectance spectra (DRS) of samples were recorded on a Varian Carry 500 Scan, equipped with an integrating sphere attachment. The reflectance data were converted to the $F(R_\infty)$ values according to Kubelka–Munk theory.[20] IR spectra were recorded in transmittance mode with a resolution of 4 cm^{-1} using a Nicolet Nexus 670 FTIR spectrometer and 20 mg of catalyst.

Electron paramagnetic resonance (EPR) signals of the radicals spin-trapped by DMPO were recorded with a Bruker ESP 300E spectrometer after 2 min irradiation of methanolic dispersions (catalyst, 4 g L^{-1}; DMPO, 0.053 M). The irradiation source (λ = 355 nm) was a Quanta-Ray Nd:YAG pulsed (10 Hz) laser system. The settings for the EPR spectrometer were: center field = 3480 G, microwave frequency = 9.79 GHz and power = 5.05 mW.

Surface photovoltage (SPV) technique, a very sensitive tool for studying the change of charge distribution on semiconductor surfaces,[21–23] buried interfaces,[24] and heterojunctions,[25,26] has successfully been applied to the investigation of electron processes in semiconductors.[27–34] The formation of photovoltage reflects directly the efficiency of photogenerated charge separation and charge-transfer across the space charge region (SCR). SPS were measured on an Edinburgh FL/FS900 spectrophotometer equipped with a lock-in amplifier (Standford, SR830-DSP) synchronized with a light chopper (Standford, SR540). A sample of 60 mg was pressed in the form of a self-supporting slice under the pressure of 6 MPa, and then placed in a photovoltaic cell of indium tin oxide (ITO)/sample/ITO sandwich structure. The photovoltaic cell was fixed in a sample chamber with quartz windows, connected to an ultra high vacuum system (KYKY Co., Beijing). Prior to the experiments, the sample was heated to 523 K for 3 h at 10^{-6} Torr, and then balanced in different gases at atmospheric pressure. Since no remarkable absorption of the ITO electrode was detected above 330 nm (see inset in Fig. 1), the photoinduced surface photovoltage spectra were obtained by scanning in the wavelength range of 330–420 nm at a resolution of 1 nm.

2.3. Photocatalytic activity measurements

The photocatalytic reactivity measurements were carried out in a fixed-bed reactor operated at atmospheric pressure. The reactor was an 11 cm long, 2.4 mm diameter, quartz tube surrounded by four 4 W UV-lamps with a wavelength centered at 254 nm (Philips, TUV 4W/G4 T5). Organic pollutants bubbled with oxygen and 7.8% hydrogen in nitrogen were fed to 0.05 g of catalyst at a total flow-rate of 50 cm^3 min^{-1}, corresponding to GHSV = 79 600 h^{-1}. The temperature of the reactions was controlled at 303 ± 1 K by an air-cooling system.

The effluent gas was analyzed by an online gas chromatograph (HP6890) equipped with a flame ionization detector (FID), a thermal conductivity detector (TCD) and a Porapak

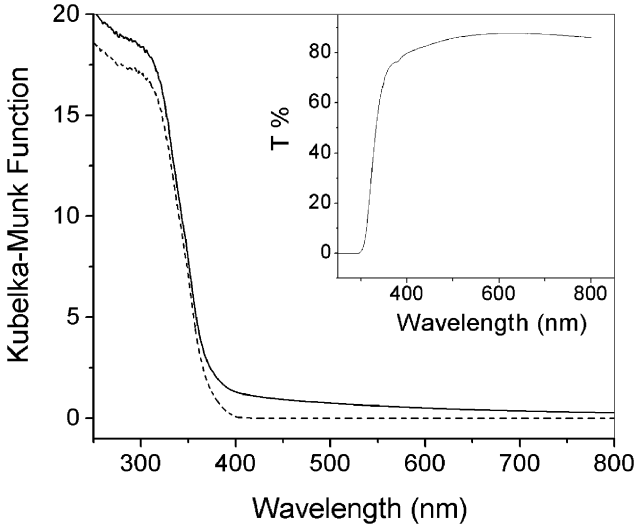

Fig. 1 Diffuse reflectance spectra of TiO_2 (dotted curve), Pt/TiO_2 (solid curve) and transmission spectrum of ITO glass (inset). The Kubelka–Munk function, $F(R_\infty) = (1 - R_\infty)^2/2R_\infty$, is used as the equivalent of absorbance.

R column. The concentrations of organic pollutants and carbon dioxide were determined by using the FID and TCD detectors, respectively. The gas chromatograph was calibrated using known concentrations of reactants and carbon dioxide. Percent mineralization of reactants was calculated by using eqn (1):

$$\%\,\text{mineralization} = \frac{[CO_2]_{\text{produced}}}{x[C_xH_y]_{\text{converted}}} \times 100 \qquad (1)$$

3. Results and discussion

3.1. Physicochemical properties of Pt/TiO_2

The XRD and N_2-sorption measurement results showed that Pt/TiO_2 and pure TiO_2 possess virtually identical textural properties, probably due to the small loading of Pt. The dominant crystal phase for Pt/TiO_2 and TiO_2 samples is anatase (85 ± 5%) with an average crystal size of 10 ± 1 nm. No diffraction peaks for the Pt dopant were detected, indicating that platinum is highly dispersed on TiO_2. The BET specific surface area (91 ± 4 m^2 g^{-1}) is the same for both Pt/TiO_2 and TiO_2. These results agree well with the literature.[14] Fig. 1 shows the diffuse reflectance spectra of Pt/TiO_2 and TiO_2. The former displayed an enhanced optical absorption throughout the detected region. This is due to the presence of Pt on TiO_2, in agreement with the black color of the powder.

3.2. Photocatalytic activity

Fig. 2a shows the photocatalytic conversion of benzene on Pt/TiO_2 in different atmospheres. In a pure H_2 atmosphere, the conversion of benzene is about zero. This is anticipated because the PCO of benzene usually requires oxygen molecules and the thermally catalytic hydrogenation of benzene occurs at high temperatures.[35] Similarly, the conversion of benzene in a pure O_2 atmosphere is also very small (3%) after reaction for 2 h, and no detectable CO_2 is observed. These results indicate that only a small amount of benzene is partially oxidized. Surprisingly, when the feeding gas contains both H_2 and O_2, the conversion of benzene increases up to 71%, accompanied by the production of a large amount of CO_2. The CO_2 yield is calibrated to be 2853 ppm, corresponding to a mineralization ratio of 78% (see Fig. 2b). It should be noted that no enhancement in photocatalytic activity is observed when water vapor (~300 ppm) is added into the O_2–Pt/TiO_2 system.

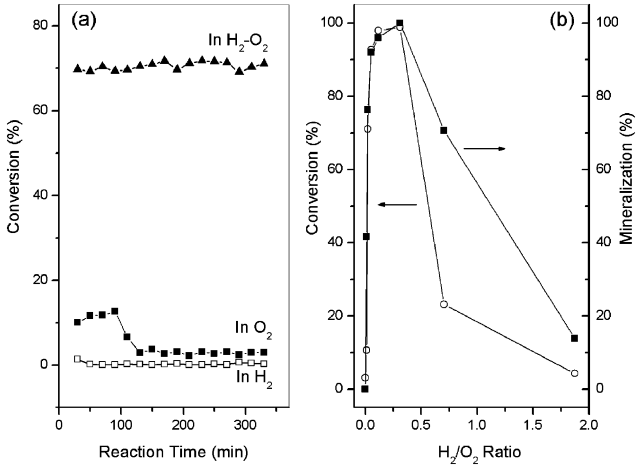

Fig. 2 (a) Effect of different reaction atmospheres on the conversion of benzene (845 ppm) on a Pt/TiO_2 photocatalyst. ($H_2:O_2$ ratio: 0.02 : 1). (b) Effect of the $H_2:O_2$ ratio on the photocatalytic performance of Pt/TiO_2 toward benzene decomposition.

Fig. 2b shows the benzene photocatalytic conversion and mineralization as a function of $H_2:O_2$ ratio. The result reveals that the photocatalytic performance of Pt/TiO_2 can be dramatically improved even with trace amounts of H_2, and is sensitive to the $H_2:O_2$ ratio. When the $H_2:O_2$ ratio increases from 0 : 1 to 0.05 : 1, the photocatalytic conversion of benzene increases rapidly from 3% to 93%. Further increasing the $H_2:O_2$ ratio from 0.05 : 1 to 0.31 : 1, the conversion steadily increases from 93% to 100% with a slower increasing rate. It is noted that the complete mineralization of benzene to CO_2 and H_2O can be achieved when the $H_2:O_2$ ratio is 0.31 : 1. However, when the $H_2:O_2$ ratio is further increased to a higher value than 0.31 : 1, significant drops of both conversion and mineralization ratios occur. These results reveal that a proper $H_2:O_2$ ratio is required for enhancing the efficiency of benzene photocatalytic oxidation over Pt/TiO_2. The optimum $H_2:O_2$ ratio is *ca.* 0.31, at which 100% benzene is completely decomposed to the final products of CO_2 and H_2O. It is not surprising that too high an $H_2:O_2$ ratio is disadvantageous to the complete degradation of benzene, because the oxidation of benzene stoichiometrically requires a large amount of O_2, and therefore, the presence of excess H_2 is unfavorable for the reaction.

Fig. 3 shows the repetition tests of the photocatalytic performance of Pt/TiO_2 towards benzene decomposition. The result demonstrates that the high photocatalytic performance of Pt/TiO_2 for the benzene oxidation is effectively maintained after 22 h of testing, by the repeated use of the catalyst four times. In every run, the steady state of the reaction, including conversion and mineralization of benzene, is achieved after 200 min.

As a comparison, we also measured the photocatalytic performances of pure TiO_2 and Pt (deposited on an insulator such as silica) under the same experimental conditions. As expected, either TiO_2 or Pt alone shows poor catalytic performance for benzene photooxidation. It is therefore believed that the interactions among TiO_2, Pt, H_2 and O_2 contribute to the superior activity and durability of Pt/TiO_2.

Fig. 4 indicates that Pt/TiO_2 also exhibits the good photocatalytic performance for the degradation of other VOCs in an H_2–O_2 atmosphere. It seems that if an alkyl (*e.g.* methyl or ethyl) is substituted onto the aromatic ring, pollutants are easier to decompose as compared with benzene. The photocatalytic conversions of toluene and ethylbenzene on Pt/TiO_2 are 83% and 90%, respectively, accompanied by a similar mineralization of 86%. As the aromatic rings with alkyl groups (methyl or ethyl) may have a higher electron cloud density on the conjugate ring, these reactant molecules may be easily bound on Pt particles and then attacked by surface active oxygen species. Contrarily, with a decrease in the electron cloud density of the cyclic six-ring, the conversion and mineralization of cyclohexane are relatively low (55% and 65%), as compared with benzene. For comparison, measurements were also obtained in a pure O_2 atmosphere. The result showed that only small amounts of these organic reactants (3–5%) were partially oxidized on Pt/TiO_2 with no CO_2 detected. This suggests that some intermediates may occupy sites on the sample and deactivate it. In addition, acetone was chosen in this study since it was detected as an intermediate of benzene photocatalytic degradation reported by Sitkiewitz *et al.*[36] Similar to the other VOCs considered, acetone can be photodegradated on Pt/TiO_2 in an H_2–O_2 atmosphere. The conversion and mineralization are 63% and 56%, respectively. However, these values decrease correspondingly to 16% and 15% when the sample is tested in a pure O_2 atmosphere. This indicates that acetone is easier to decompose on Pt/TiO_2 than the other reactants in the absence of H_2.

All of the above photocatalytic activity experiments were carried out with UV-254 nm irradiation. To further confirm the effect of H_2 on benzene photooxidation over Pt/TiO_2, another kind of UV lamp (Philips, TL 4W 105) with a wavelength centered at 365 nm was used as the irradiation source. Fig. 5 shows that the conversion and mineralization of benzene are *ca.* 57% and 67%, respectively, which are slightly lower than those found on using 254 nm lamps (see Fig. 2a). This discrepancy in efficiency is produced by the different irradiation energy, because the UV intensity of 365 nm lamps

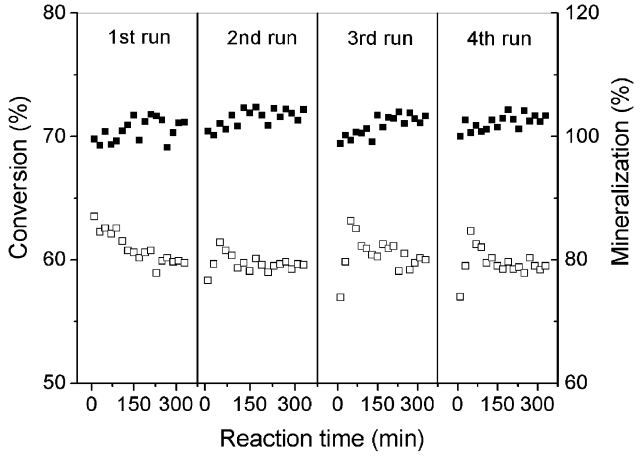

Fig. 3 Cycling runs for the photooxidation of benzene on Pt/TiO_2 in an H_2–O_2 atmosphere ($H_2:O_2$ ratio: 0.02 : 1). Symbols ■ and □ represent conversion and mineralization of benzene, respectively.

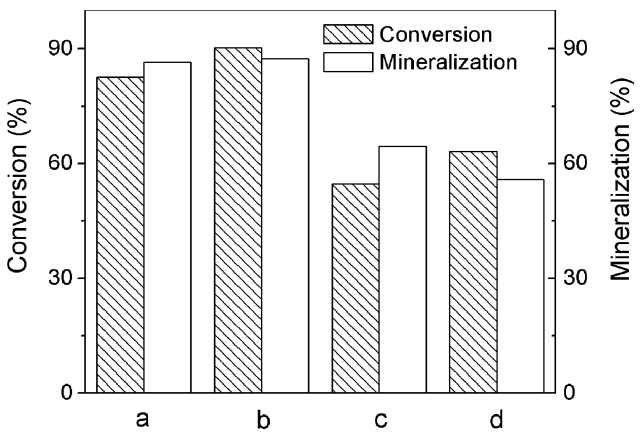

Fig. 4 Photooxidation of different pollutants on Pt/TiO_2 in an H_2–O_2 atmosphere ($H_2:O_2$ ratio: 0.02 : 1): (a) toluene (852 ppm), (b) ethylbenzene (848 ppm), (c) cyclohexane (856 ppm) and (d) acetone (853 ppm).

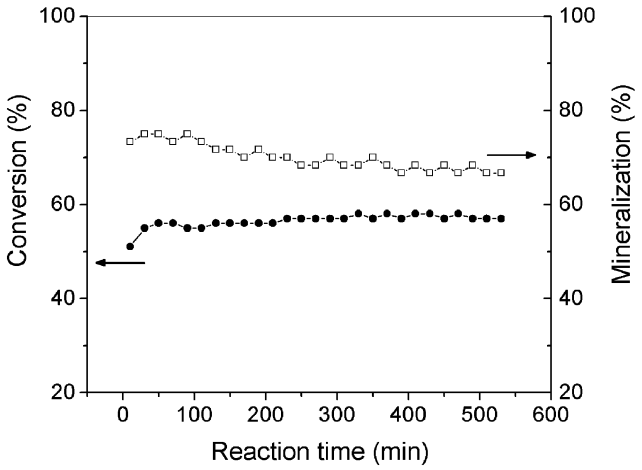

Fig. 5 Photocatalytic oxidation of benzene on Pt/TiO_2 with 365 nm lamps in the presence of H_2–O_2 (H_2 : O_2 ratio: 0.02 : 1).

(0.7 mW cm^{-2}) is lower than that of 254 nm lamps (2.1 mW cm^{-2}).

3.3. IR spectra

Fig. 6 displays the IR spectra of a Pt/TiO_2 sample before and after benzene photooxidation in different atmospheres. Obviously, deposits on the surface of the sample are found to depend on the atmosphere. In an O_2 atmosphere, a small band at 1487 cm^{-1}, which is assigned to an aromatic ring stretching vibration,[37] shows depositing of some aromatic compounds on the surface. This band can be better identified by the corresponding difference IR spectra (see Fig. 6 inset). Because of enveloping by the stronger adsorption of the absorbed water and/or hydroxyl groups, no other characteristic bands of aromatic rings are observed in the range 1500–1620 cm^{-1}. The bands at *ca.* 1206 cm^{-1} and in the range of 1260–1410 cm^{-1} are assigned to the O–H deformation vibration of phenolic compounds.[37,38] Sasaki *et al.* have reported that the reaction of $^{\bullet}OH$ radical with benzene in the presence of oxygen results in the main products of phenol and benzoquinone in the molar ratio *ca.* 10 : 1.[39] So, it seems reasonable that this hydroxylation of benzene occurs in the photocatalytic process. The hydroxylation is caused by the active $^{\bullet}OH$ radical which is generated from the oxidation of a surface hydroxyl on Pt/TiO_2 by a photogenerated hole.[40] Moreover, Bellamy has suggested that the appearance of a characteristic band in the range of 1170–1140 cm^{-1} is related to the *meta*-substitution of an aromatic ring.[37] In the O_2 atmosphere, as surface hydroxyl groups are consumed to produce phenol, the probability for the direct oxidation of benzene by the photogenerated hole may be increased [eqn (2)].[41] The resulting benzene cation, a strong electron acceptor,[42–44] subsequently causes the *meta*-substitution of phenol [eqn (3)]. This addition reaction may thus lead to the formation of stable aromatic intermediates, which deactivate the Pt/TiO_2 photocatalyst.[17]

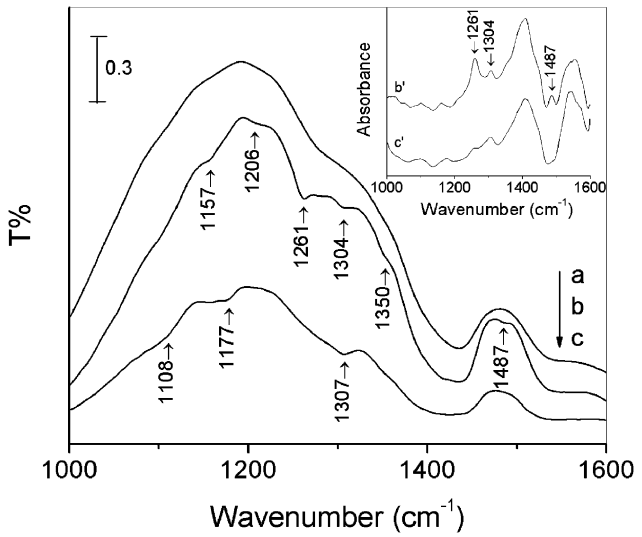

Fig. 6 IR spectra of a Pt/TiO_2 sample in different atmospheres: (a) before benzene photooxidation; (b) after benzene photooxidation in O_2 for 6 h; (c) after benzene photooxidation in H_2–O_2 (H_2 : O_2 ratio: 0.02 : 1) for 6 h. The inset shows the difference IR spectra: $b' = (b - a)$ and $c' = (c - a)$.

Interestingly, no obvious aromatic products are detected on the catalyst surface after the reaction in an H_2–O_2 atmosphere (see Fig. 6c). The band at 1307 cm^{-1} can be assigned to an in-plane O–H deformation vibration, and the band at 1307 cm^{-1} and 1108 cm^{-1} can be assigned to the C–O stretch mode of alcohols or ethers.[38] It appears that the cleavage of benzene rings takes place and some alcohols or ethers are produced as intermediates on Pt/TiO_2. It deserves to be mentioned that this anti-deactivation property for the platinized TiO_2 is obtained by adding trace H_2 into the O_2-rich photooxidation system. This may be explained by the dissociative adsorption of H_2 on the surfaces of the Pt particles to form H adatoms.[45] Because the H adatom is a stronger hole acceptor compared with benzene, it can be easily oxidized by the photogenerated hole of TiO_2, thus may inhibit the formation of benzene cations and the subsequent aromatic intermediates. Moreover, owing to their small size and high mobility, the H adatoms may significantly perturb the metal surface structure, inducing reconstruction/cleaning of the metal surface.[46–48] This may also account for the long catalytic lifetime of Pt/TiO_2 in an H_2–O_2 atmosphere.

$$C_6H_6 + h^+ \rightarrow C_6H_6^+ \quad (2)$$

$$C_6H_6^+ + C_6H_5OH \rightarrow (C_6H_6\text{–}C_6H_5OH)^+ \quad (3)$$

3.4. EPR and SPS spectra

As suggested by the results of the IR tests, the photoreactions on Pt/TiO_2 in O_2 and H_2–O_2 atmospheres follow different mechanisms, and the formation of $^{\bullet}OH$ radicals plays an important role in the degradation process of the aromatic compounds. Using DMPO as a spin-trapping reagent, information about active radicals can be obtained by the spin-trapping EPR technique (see Fig. 7). It is evident that some

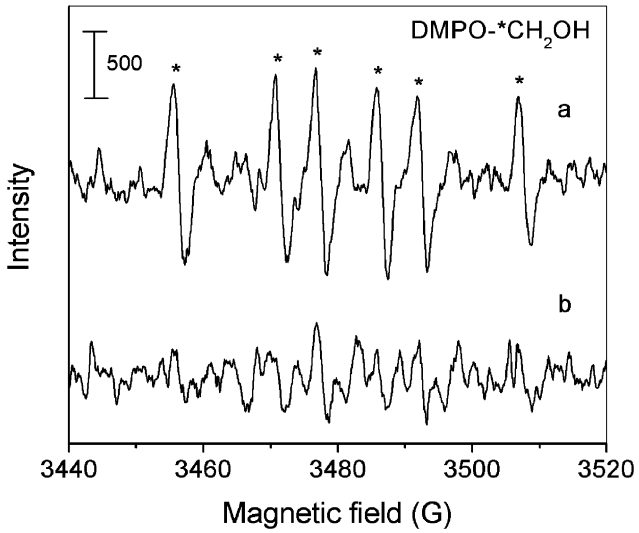

Fig. 7 Spin-trapping EPR spectra of methanolic dispersions containing Pt/TiO_2 and DMPO in the presence of (a) H_2–O_2 (H_2 : O_2 ratio: *ca.* 1.0 : 1) and (b) O_2.

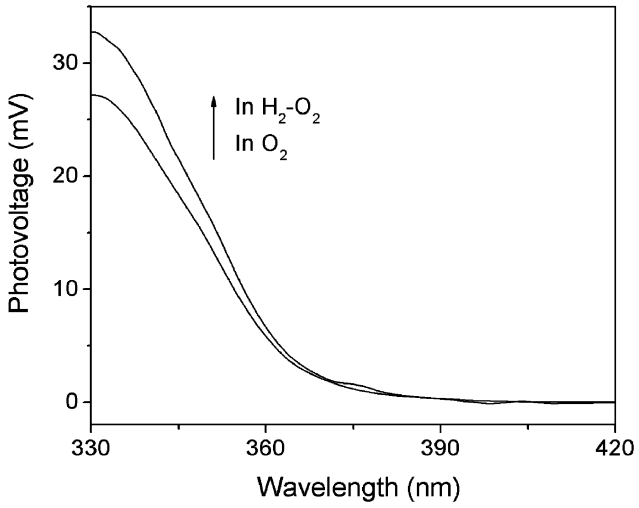

Fig. 8 SPS of Pt/TiO_2 in O_2 and H_2–O_2 atmospheres (H_2 : O_2 ratio: 0.02 : 1).

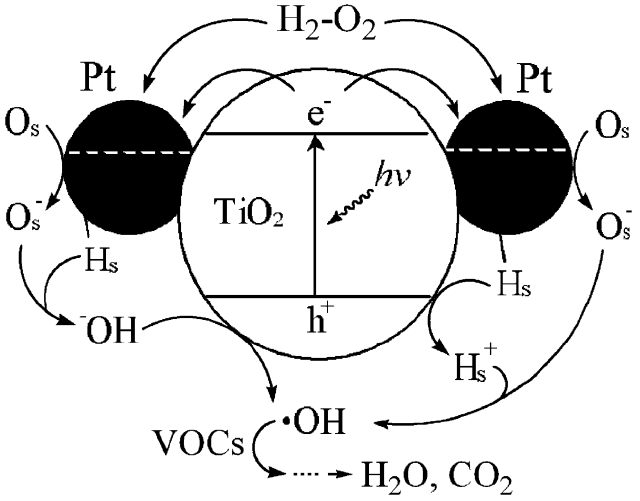

Scheme 1 Proposed mechanism for the photochemical generation of $^\bullet OH$ radicals on a Pt/TiO_2 catalyst in the coexistence of H_2 and O_2.

active radicals are photogenerated on Pt/TiO_2 in O_2 and H_2–O_2 atmosphere. When the system contains both H_2 and O_2, six strong peaks are clearly observed (see Fig. 7a). These characteristic peaks can be assigned to the DMPO–$^\bullet CH_2OH$ adducts originating from the attack of $^\bullet OH$ radicals on the methanol molecules [see eqn (4)].[49,50] The result demonstrates that large numbers of $^\bullet OH$ radicals are produced in this process, confirming the beneficial effect of H_2–O_2 in the photocatalytic oxidation of the organic pollutants. However, when exposed to pure oxygen, though some active radicals are also produced, they are too weak to identify. This indicates that the generation efficiency of active radicals is much lower in the O_2–Pt/TiO_2 photocatalytic system than that in the H_2–O_2–Pt/TiO_2 photocatalytic system. In addition, Fig. 7b also supports the conclusion that oxygen is dissociatively adsorbed on Pt/TiO_2 since no obvious DMPO–$O_2^{-\bullet}$ peaks are found.[45,50]

$$^\bullet OH + CH_3OH \rightarrow {}^\bullet CH_2OH + H_2O \quad (4)$$

Fig. 8 displays the SPS of Pt/TiO_2 in O_2 and H_2–O_2 atmospheres. Obviously, ranging from 370 nm to 330 nm, an increasing SPV response is obtained by adding trace H_2 into the O_2–Pt/TiO_2 system. The result suggests that the separation efficiency of photogenerated electron–hole pairs in the H_2–O_2–Pt/TiO_2 system is higher than that in the O_2–Pt/TiO_2 system. This may, in principle, contribute to the high photocatalytic activity of Pt/TiO_2 for decomposing persistent organic pollutants in an H_2–O_2 atmosphere.[51] It is not surprising that the higher separation efficiency is obtained by adding trace H_2 into the O_2 atmosphere, because the $^\bullet OH$ radical formed in H_2–O_2 has a higher electron-affinity than that of the O adatom produced in O_2 ($^\bullet OH/^-OH$: 1.828 eV, O/O^-: 1.478 eV).[52,53]

3.5. Discussion

Based on the above experimental results, the photochemical processes in the H_2–O_2–Pt/TiO_2 reaction system are proposed and elucidated in Scheme 1 and eqn (5)–(10).[18] These processes may involve several steps: (a) O_2 and H_2 dissociatively adsorb on Pt particles to give surface O (O_s) and surface H (H_s) adatoms. (b) The resulting O_s adatom captures a photogenerated electron from the Pt particles, producing an O_s^- ion. (c) The H_s adatom migrates from Pt to the interface of $Pt\|TiO_2$,[54] and then serves as a trapping agent for the hole, generating a surface proton (H_s^+) which further reacts with the O_s^- ion to give a highly active $^\bullet OH$ group. (d) The O_s^- ion could also react with the H_s adatom to produce ^-OH that also captures h^+, leading to the formation of $^\bullet OH$ radicals. These four processes are believed to generate a large number of $^\bullet OH$ groups, which is proved by the spin-trapping EPR spectra. Since the oxidative degradation of organic compounds such as benzene is initiated by $^\bullet OH$,[55] a large increase in the photocatalytic activity is possible. However, as the excess H_2 would consume the produced hydroxyl radicals [eqn (11)], this results in the consequent decrease in the conversion (see Fig. 2b). Although eqn (12) may also produce $^\bullet OH$ radicals,[56,57] we found that this non-photogenerated $^\bullet OH$ has only a slight effect on the overall catalytic performance, as revealed by the oxidation of benzene on Pt/TiO_2 in the dark.

$$TiO_2 + UV \rightarrow e^- + h^+ \quad (5)$$

$$O_s\text{–}Pt + e^- \rightarrow O_s^- \quad (6)$$

$$H_s\text{–}Pt + h^+ \rightarrow H_s^+ \quad (7)$$

$$O_s^- + H_s^+ \rightarrow {}^\bullet OH \quad (8)$$

$$O_s^- + H_s\text{–}Pt \rightarrow {}^-OH \quad (9)$$

$$^-OH + h^+ \rightarrow {}^\bullet OH \quad (10)$$

$$H_s\text{–}Pt + {}^\bullet OH \rightarrow H_2O \quad (11)$$

$$O_s\text{–}Pt + H_s\text{–}Pt \rightarrow {}^\bullet OH \quad (12)$$

Furthermore, it is noted that the interfacial electron-transfer on the photocatalyst surface is a rate-determining step during the photocatalytic reactions.[51] Normally, the interfacial electron-transfer is accomplished by capturing the electron at surface-adsorbed O_2 on the TiO_2 photocatalyst.[51] As the electron-affinity of the O adatom (O/O^-, 1.478 eV) is much higher than that of O_2 (O_2/O_2^-, 0.43 eV),[53,58] the O adatom should be a superior trapping agent for the electron [eqn (6)], as compared with O_2. Subsequent capturing of the resulting O_s^- ion by H_s^+/H_s [eqn (8) and (9)] could further favor the interfacial electron transfer. An increase in the interfacial electron-transfer rate is expected to result in higher quantum efficiencies for the photocatalytic reactions.

In the H_2–O_2–Pt/TiO_2 system, the mechanism for the photodegradation of stable organic pollutants significantly differs from that in the O_2–Pt/TiO_2 system. In the latter, the quantity of surface hydroxyl groups on the catalyst is limited, and the surface hydroxyl groups are consumed to form some phenolic compounds without any regeneration during the reaction. This may cause the deactivation of Pt/TiO_2, as proved by IR spectra. In the H_2–O_2–Pt/TiO_2 system, however, the H adatoms on Pt/TiO_2 are active for the photogeneration of $^\bullet OH$ radicals. This continuous formation of $^\bullet OH$ radicals may thus

contribute to the high photocatalytic activity and durability of Pt/TiO_2.

4. Conclusions

Superior photocatalytic activity and stability of Pt/TiO_2 for decomposing benzene have been obtained by adding trace H_2 into an O_2-rich photooxidation system. The H_2–O_2–Pt/TiO_2 photocatalytic system was also successfully applied to decompose some other persistent VOCs. The order of photodegradation efficiencies is cyclohexane < acetone < benzene < toluene < ethylbenzene. The promotion effects of H_2 during photodegradation of organic pollutants on Pt/TiO_2 can be interpreted as (i) suppressing the deposition of persistent aromatic intermediates on the catalyst; (ii) promoting the formation of surface hydroxyl radicals in the photocatalytic process; (iii) improving the separation efficiency of photogenerated electron–hole pairs on Pt/TiO_2.

Acknowledgements

This work is financially supported by the National Natural Science Foundation of China (20133010, 20273014, 20473018, 20573020 and 20537010), Key Foundation of Science and Technology of MOE, China (03061 and JA02138), and the Natural Science Foundation of Fujian, China (2003F004).

References

1 R. M. Alberic and W. F. Jardim, *Appl. Catal., B*, 1997, **14**, 55.
2 M. L. Sauer and D. F. Ollis, *J. Catal*., 1996, **163**, 215.
3 L. A. Dibble and G. B. Raupp, *Environ. Sci. Technol*., 1992, **26**, 492.
4 L. Cao, Z. Gao, S. L. Suib, T. N. Obee, S. O. Hay and J. D. Freihaut, *J. Catal*., 2000, **196**, 253.
5 J. Peral and D. F. Ollis, *J. Catal*., 1992, **136**, 554.
6 M. M. Ameen and G. B. Raupp, *J. Catal*., 1999, **184**, 112.
7 H. Einaga, S. Futamura and T. Ibusuki, *Chem. Lett*., 2001, 582.
8 N. Schrauzer and T. D. Guth, *J. Am. Chem. Soc*., 1977, **99**, 7189.
9 R. Baba, S. Nakabayashi, A. Fujishima and K. Honda, *J. Phys. Chem*., 1985, **89**, 1902.
10 A. Heller, *Pure Appl. Chem*., 1986, **58**, 1189.
11 K. Domen, Y. Sakata, A. Kudo, K. Maruya and T. Onishi, *Bull. Chem. Soc. Jpn*., 1988, **61**, 359.
12 M. Anpo, K. Chiba, M. Tomonari, S. Coluccia, M. Che and M. A. Fox, *Bull. Chem. Soc. Jpn*., 1991, **64**, 543.
13 A. J. Bard and M. A. Fox, *Acc. Chem. Res*., 1995, **28**, 7985.
14 X. Z. Fu, W. A. Zeltner and M. A. Anderson, *Appl. Catal., B*, 1995, **6**, 209.
15 X. Z. Fu, Z. X. Ding and W. Y. Su, *Chin. J. Catal*., 1999, **20**, 321.
16 J. L. Falconer and K. A. Magrini-Bair, *J. Catal*., 1998, **179**, 171.
17 S. A. Larson and J. L. Falconer, *Catal. Lett*., 1997, **44**, 57.
18 Y. Chen, D. Li, X. Wang, X. Wang and X. Fu, *Chem. Commun*., 2004, 2304.
19 X. Z. Fu, W. A. Zeltner, Q. Yang and M. A. Anderson, *J. Catal*., 1997, **168**, 428.
20 G. Kortum, *Reflectance Spectroscopy*, Springer-Verlag, New York, 1969.
21 L. Kronik and Y. Shapira, *Surf. Sci. Rep*., 1999, **37**, 1.
22 I. Baikie, U. Petermann and B. Lägel, *Surf. Sci*., 1999, **433–435**, 249.
23 I. Shalish, Y. Shapira, L. Burstein and J. Salzman, *J. Appl. Phys*., 2001, **89**, 390.
24 B. Lägel, I. D. Baikie and U. Petermann, *Surf. Sci*., 1999, **433–435**, 622.
25 L. S. Li, J. Zhang, L. J. Wang, Y. Chen, Z. Hui, T. J. Li, L. F. Chi and H. Fuchs, *J. Vac. Sci. Technol., B*, 1997, **15**, 1618.
26 H. Du, Y. Cao, Y. Bai, P. Zhang, X. Qian, D. Wang, T. Li and X. Tang, *J. Phys. Chem. B*, 1998, **102**, 2329.
27 D. Gal, Y. Mastai, G. Hodes and L. Kronok, *J. Appl. Phys*., 1999, **86**, 5573.
28 A. D. Q. Li and L. S. Li, *J. Phys. Chem. B*, 2004, **108**, 12842.
29 T. Xie, D. Wang, L. Zhu, C. Wang, T. Li, X. Zhou and M. Wang, *J. Phys. Chem. B*, 2000, **104**, 8177.
30 L. S. Li, Q. X. Jia and A. D. Q. Li, *Chem. Mater*., 2002, **14**, 1159.
31 Y. Lin, D. Wang, Q. Zhao, M. Yang and Q. Zhang, *J. Phys. Chem. B*, 2004, **108**, 3202.
32 T. He, Y. Ma, Y. Cao, P. Jiang, X. Zhang, W. Yang and J. Yao, *Langmuir*, 2001, **17**, 8024.
33 M. Qi and G. Liu, *J. Phys. Chem. B*, 2003, **107**, 7640.
34 D. Wang, Y. Cao, X. Zhang, Z. Liu, X. Qian, X. Ai, F. Liu, D. Wang, Y. Bai, T. Li and X. Tang, *Chem. Mater*., 1999, **11**, 392.
35 R. V. Kazantsev, N. A. Gaidai, N. V. Nekrasov, K. Tenchev, L. Petrov and A. L. Lapidus, *Kinet. Catal*., 1998, **39**, 363.
36 S. Sitkiewitz and A. Heller, *New J. Chem*., 1996, **20**, 233.
37 L. J. Bellamy, *The Infra-red Spectra of Complex Molecules*, Chapman and Hall, London, 1975.
38 D. H. Williams and I. Fleming, *Spectroscopic Methods in Organic Chemistry*, McGraw-Hill Book Company (UK) Limited, London, 1987.
39 A. Kunai, S. Hata, S. Ito and K. Sasaki, *J. Am. Chem. Soc*., 1986, **108**, 6012.
40 M. Anpo, T. Shima and Y. Kubokawa, *Chem. Lett*., 1985, 1799.
41 H. Einaga, S. Futamura and T. Ibusuki, *Phys. Chem. Chem. Phys*., 1999, **1**, 4903.
42 T. Komatsu and A. Lund, *J. Phys. Chem*., 1972, **76**, 1727.
43 A. F. Bedilo, V. I. Kim and A. M. Volodin, *J. Catal*., 1998, **176**, 294.
44 Y. Kurita, T. Sonoda and M. Sato, *J. Catal*., 1970, **19**, 82.
45 D. O. Hayward and B. M. W. Trapnell, *Chemisorption*, Butterworths, London, 1964.
46 S. Penner, D. Wang, D. S. Su, G. Rupprechter, R. Podloucky, S. Schlögl and K. Hayek, *Surf. Sci*., 2003, **532–535**, 276.
47 B. Delmon, in *Studies in Surface Science and Catalysis 77*, ed. T. Inui, K. Fujimoto, T. Uchijima and M. Masai, Elsevier, Kyoto, Japan, 1933.
48 H. Chen and J. M. White, *J. Mol. Catal*., 1986, **35**, 355.
49 W. Zhao, C. Chen, X. Li and J. Zhao, *J. Phys. Chem. B*, 2002, **106**, 5022.
50 T. Wu, G. Liu, J. Zhao, H. Hidaka and N. Serpone, *New J. Chem*., 2000, **24**, 93.
51 M. R. Hoffmann, S. T. Martin, W. Choi and D. W. Bahnemann, *Chem. Rev*., 1995, **95**, 69.
52 *CRC Handbook of Chemistry and Physics*, ed. D. R. Lide, CRC Press, Florida, 86th edn, 2005–2006.
53 R. S. Berry, J. C. Mackie, R. L. Taylor and R. Lynch, *J. Chem. Phys*., 1965, **43**, 3067.
54 E. V. Benvenutti, L. Franken, C. C. Moro and C. U. Davanzo, *Langmuir*, 1999, **15**, 8140.
55 G. Ghigo and G. Tonachini, *J. Am. Chem. Soc*., 1999, **121**, 8366.
56 T. Hayashi, K. Tanaka and M. Haruta, *J. Catal*., 1998, **178**, 566.
57 W. R. Williams, C. M. Marks and L. D. Schmidt, *J. Phys. Chem*., 1992, **96**, 5922.
58 J. L. Pack and A. V. Phelps, *J. Chem. Phys*., 1966, **44**, 1870.